UNIVERSITY of York

This is a repository copy of X-ray phase-contrast imaging for laser-induced shock waves.

White Rose Research Online URL for this paper: <u>https://eprints.whiterose.ac.uk/146341/</u>

Version: Accepted Version

Article:

Antonelli, L. orcid.org/0000-0003-0694-948X, Barbato, F., Mancelli, D. et al. (14 more authors) (2019) X-ray phase-contrast imaging for laser-induced shock waves. EPL. 35002. ISSN 1286-4854

https://doi.org/10.1209/0295-5075/125/35002

Reuse

This article is distributed under the terms of the Creative Commons Attribution-NonCommercial-NoDerivs (CC BY-NC-ND) licence. This licence only allows you to download this work and share it with others as long as you credit the authors, but you can't change the article in any way or use it commercially. More information and the full terms of the licence here: https://creativecommons.org/licenses/

Takedown

If you consider content in White Rose Research Online to be in breach of UK law, please notify us by emailing eprints@whiterose.ac.uk including the URL of the record and the reason for the withdrawal request.



eprints@whiterose.ac.uk https://eprints.whiterose.ac.uk/

X-ray phase-contrast imaging for laser-induced shock waves

L. ANTONELLI^{1,2}, F. BARBATO³, D. MANCELLI^{4,5}, J. TRELA⁴, G. ZERAOULI^{6,7}, G. BOUTOUX⁴, P NEUMAYER⁸, S. ATZENI¹, A. SCHIAVI¹, L. VOLPE^{6,7}, V. BAGNOUD⁸, C. BRABETZ⁸, B. ZIELBAUER⁸, P. BRADFORD², N. WOOLSEY², B. BORM⁹ and D. BATANI⁴

¹ Dipartimento SBAI, Università degli Studi di Roma "La Sapienza", Via Antonio Scarpa 14, 00161, Roma, Italy

² York Plasma Institute, Department of Physics, University of York, York, YO10 5DQ, United Kingdom

³ Empa - Swiss Federal Laboratories for Materials Science and Technology, Überlandstrasse 129, CH8600 Dübendorf, Switzerland

⁴ Université de Bordeaux, CNRS, CEA, CELIA (Centre Lasers Intenses et Applications), UMR 5107, F-33405 Talence, France

⁵ University of the Basque Country (UPV/EHU), Donostia International Physics Center (DIPC), Donostia/San Sebastin, Basque Country, Spain

⁶ CLPU, Centro de Láseres Pulsados, Edificio M5. Parque Científico. C/ Adaja, 8. 37185 Villamayor, Salamanca, Spain

⁷ Universidad de Salamanca Facultad de Ciencias. Plaza de los Caídos, s/n. 37008 Salamanca, Spain

⁸ GSI Helmholtzzentrum für Schwerionenforschung GmbH, Planckstraße 1, 64291 Darmstadt, Germany

⁹ Goethe-Universität Frankfurt, Max-von-Laue-Straße 1, 60438 Frankfurt am Main, Germany

PACS 52.50.Lp – Heating plasma by shock-wave
PACS 52.38.Mf – Laser ablation laser-plasma interactions
PACS 87.59.-e – X-ray imaging

Abstract – X-ray phase-contrast imaging (XPCI) is a versatile technique with applications in many fields, including fundamental physics, biology and medicine. Where X-ray absorption radiography requires high density ratios for effective imaging, the image contrast for XPCI is a function of the density gradient. In this letter, we apply XPCI to the study of laser-driven shock waves. Our experiment was conducted at the Petawatt High-Energy Laser for Heavy Ion EXperiments (PHELIX) at GSI. Two laser beams were used: one to launch a shock wave and the other to generate an X-ray source for phase-contrast imaging. Our results suggest that this technique is suitable for the study of warm dense matter (WDM), inertial confinement fusion (ICF) and laboratory astrophysics.

X-ray phase contrast imaging (XPCI) is based on the 1 phase-shift of X-ray photons induced by a density gradi-2 ent. In the presence of a density variation, the incident X-3 ray photons are deflected from higher density to lower den-4 sity regions, generating an intensity fringe at the gradient. 5 Synchrotrons and Free Electron Lasers are ideal experi-6 mental platforms for XPCI because they can deliver coherent radiation at high energy (to accentuate the phase-shift 8 and limit photon absorption) and high flux [1-3]. It is also possible to use broadband incoherent radiation for phase 10 contrast imaging, however the corresponding X-ray source 11 must be very small. One method for generating small-scale 12 X-ray sources suitable for XPCI is to use laser-irradiated 13 solid targets [4, 5]. XPCI has already made an important 14

contribution to the fields of biology and medicine [6–9], 15 but laser-driven XPCI could also be applied to studies of 16 warm dense matter (WDM), laboratory astrophysics and 17 inertial confinement fusion (ICF). The sensitivity of XPCI 18 to density gradients means it can probe a range of differ-19 ent densities in the same measurement. This is useful for 20 studying hydrodynamic processes at material interfaces, 21 such as the Richtmyer - Meshkov and Kelvin - Helmholtz 22 instabilities. What is more, since laser-driven XPCI uses 23 a high-energy probe, it is also possible to study radiative 24 phenomena relevant to astrophysics. Large-scale laser fa-25 cilities such as the National Ignition Facility (NIF) [10] 26 and Laser Mégajoule (LMJ) [11] enable us to study mat-27 ter in extreme conditions and both have dedicated beam-28

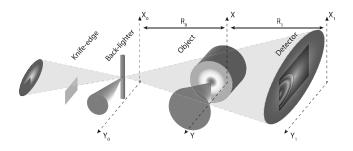


Fig. 1: Experimental set-up showing the short-pulse back-lighter and long-pulse drive beams.

lines for target probing: the Advanced Radiographic Ca-29 pability (ARC) [12] and the PETawatt Aquitaine Laser 30 (PETAL) [13]. With the increased precision and detail 31 available through XPCI, the development of XPCI lines 32 on these facilities could open up new possibilities in diag-33 nostic imaging. Though laser-driven X-ray absorption ra-34 diography has been successfully demonstrated on many ex-35 periments (some examples are reported in [14–20]), XPCI 36 using laser-produced X-ray sources has been less inten-37 sively studied. A significant advance in the application of 38 laser-driven bremsstrahlung X-ray sources to XPCI was 39 shown by Workman et al. in 2010 [21], however the qual-40 ity of the images they obtained did not allow for a com-41 prehensive study of shock wave characteristics. In [22], 42 a numerical study of cryogenic beryllium capsules using 43 phase-contrast imaging is presented, however a proof-of-44 principle laser experiment is necessary to pin down the 45 requirements of a single-shot, laser-produced X-ray source 46 for XPCI. In this letter we present the results of an exper-47 iment at the PHELIX facility [23] where XPCI was used 48 to study a laser-induced shock-wave. The total energy de-49 livered by the laser was 50 J, divided equally between the 50 short pulse beam (to generate the X-ray source) and the 51 long pulse beam (to drive the shock wave). The experi-52 mental layout can be seen in Figure 1. 53

A 25 J, 0.5 ps, 1.06 μ m wavelength laser pulse was fo-54 cussed onto a tungsten wire with a 5 μ m focal spot, lead-55 ing to on-target intensities of around $6 \times 10^{19} \text{ Wcm}^{-2}$. 56 Under these conditions, a large portion (~ 10 - 20%) 57 of the incident laser energy is transferred to relativistic 58 electrons [24] that propagate through the wire and emit 59 bremsstrahlung radiation. These hot electrons were mon-60 itored using a bremsstrahlung cannon and highly oriented 61 pyrolytic graphite (HOPG) crystal spectrometer. A knife 62 edge was used to characterize the source dimensions on 63 each shot. In the horizontal direction, the source was 64 measured to be 5 μ m across (the same as the wire diam-65 eter), while the size measured along the wire was 30 μ m. 66 The characteristics of our X-ray source are consistent with 67 phase-contrast enhancement. If we assume Fresnel diffrac-68 tion, the recorded pattern on the detector surface results 69 from the superposition of waves coming from a coherence 70 area commensurate with the transversal coherence length, 71 l_t , which is the minimum distance between two points in 72

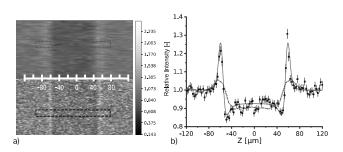


Fig. 2: a) XPCI image of plastic wires. The upper part corresponds to the IP detector while the lower part corresponds to the CCD. b) X-ray transmission profile from experimental CCD image (black dots) and synthetic profile (red line). The blue dot-dashed line is the corresponding layout on the IP from the upper part of the image (dashed blue line).

the transverse direction with a correlated phase, defined as:

$$l_t \approx \frac{R_0 \lambda}{s} \tag{1}$$

73

74

89

90

91

92

93

94

95

96

97

98

99

where R_0 is the distance from source to sample, s is the 75 source size (in our case l_t has a different value in the verti-76 cal and horizontal directions due to the source geometry) 77 and λ is the X-ray wavelength. In other words, l_t has to 78 be larger than the scale length for the structure to be re-79 solved. In the case of a laser-induced shock wave, l_t should 80 be of the order of a few microns. Equation 1 gives a crite-81 rion to evaluate a source for XPCI which is more restricted 82 than reality [25]. Taking the source dimensions into ac-83 count, the X-ray wavelength ranged from 1.2 to 2.0 Å, and 84 the distance R_0 was 24.5 cm, the minimum value of l_t is 85 1 μ m in the vertical direction and its maximum is 10 μ m 86 in the horizontal direction (where the source size is limited 87 to 5 μ m). 88

A 25 J, 2 ns, 1.06 μ m wavelength laser pulse was used to launch a shock wave in a plastic (C_8H_8) cylinder with a diameter of 300 μ m. With a focal spot diameter of 50 μ m, the intensity was about 3×10^{14} W/cm². We used two different detectors to record our images: an Image Plate (IP) and Andor CCD camera. To remove any contribution coming from the interaction of the long pulse with the target, a 500 μ m-thick Polymethyl methacrylate (PMMA) window and a 40 μ m thick Al filter were placed in front of our detectors. The transmission of these filters ranged from 2% at 5 keV to 63% at 10 keV.

We tested our set-up by imaging cylindrical nylon wires 100 with diameters from 120 to 400 μ m. The results are shown 101 in Figure 2. The image shows the presence of phase con-102 trast at the edges of the wire and low levels of absorption 103 (around 10% of the incident X-ray radiation below 5 keV). 104 If we consider the transverse profile of one of the wire 105 with respect to the wire axis (represented by black dots 106 in Figure 2b), the phase contrast edges are clearly visible 107 while absorption plays a minor role. The red line in Figure 108 2b is the synthetic profile calculated using our own code. 109 The code was designed to calculate X-ray absorption and 110

phase contrast, taking into account the X-ray spectrum, 111 source size and spatial intensity distribution and solving 112 the Kirchoff-Fresnel equation using the Fresnel approxi-113 mation [26]. The code works in cylindrical geometry and 114 it takes into account the source spectra, source size and 115 detector resolution in a similar way as described in [27, 28]. 116 Moreover, the density map associate to the object has to 117 be provided. We used the mass absorption coefficient for 118 cold Nylon available in the NIST database [29]. Consider-119 ing the experimental limitations (detector resolution, low 120 photon flux, etc.) there is good agreement between ex-121 periment and simulation. The blue dot-dashed lines cor-122 respond to a layout of the same wire on the IP. Some of 123 the details are lost due to the lower resolution, as evinced 124 by the lower ratio between the diffraction peak maximum 125 and source intensity. The amplitude of the error bars is 126 calculated from analysis of fluctuations in source intensity. 127 In Figure 3a, we observe a laser-driven shock wave prop-128 agating inside a plastic cylinder. This image was taken 8 129 ns after the end of the driving pulse using IP as detector. 130 There is evidence of both absorption and phase-contrast 131 processes, with the strongest phase-contrast at the target-132 vacuum edge (P3) and inside the shocked region (P2). 133 It is also present on the shock wave front (compressed-134 uncompressed interface, P1). XPCI is sensitive to den-135 sity variations and can provide information on shock wave 136 propagation even at moderate laser intensity. The X-ray 137 intensity inside the shock wave is higher than the vac-138 uum background intensity, suggesting that a strong den-139 sity gradient is present in the low-density region before 140 the shock front (P2). To model this internal structure, 141 we ran a number of simulations using the hydrodynamic 142 code DUED [30] coupled to the bespoke XPCI simulation 143 code. As for the nylon wires, we again assumed cold opac-144 ity for the Polystyrene. Indeed, the 5 - 10 keV backlighter 145 photons are mainly absorbed by the K-shell electrons in 146 the carbon atoms if they are not fully ionized. The typ-147 ical temperature of shock target at this intensity is few 148 eV, with a low degree of ionization. In such case the use 149 of cold opacity leads to an error no more than 1% [31]. 150 The synthetic radiograph is remapped in a lower resolu-151 tion image to match the experimental resolution. Initially, 152 we assumed a super-Gaussian focal intensity distribution 153 with a diameter of 50 μ m, a square time shape with a 154 pulse duration of 2 ns and an energy of 25 J (correspond-155 ing to the nominal parameters of the laser). Numerical 156 noise calculated from the experimental measurement was 157 added to simulation. The experimental noise is measured 158 directly on the experimental data where the target is not 159 present. Intensity oscillation follows a Gaussian behaviour 160 with a FWHM equal to 10%. A deviation from the sim-161

ulated intensity following such a behaviour is then added
to the synthetic radiograph. The results are shown in Figure 3b. Although reducing the energy in the simulation
allowed us to match the position of the wavefront on-axis,
the synthetic image looks quite different from the experimental data. Moreover the phase contrast at the simu-

lated shock front is higher than in the experiment, which 168 implies that these simulations have unrealistically steep 169 density gradients. Figure 4a shows the intensity profile 170 along the horizontal axis (to help reduce noise, the cen-171 tral line was averaged with the two nearest points in the 172 transverse direction). The numerical profiles were taken 173 without numerical noise. In this case we introduced the 174 error bar on the experimental data. Our code reproduces 175 the peak corresponding to the vacuum-target interface and 176 also the position of the shock front. The peak intensity is 177 different, however, and we can deduce that the simulation 178 is predicting a higher density-ratio between the shocked 179 and unshocked regions since the width of the simulated 180 and experimental peaks is comparable. Though signifi-181 cant phase-contrast is visible inside the simulated shock, 182 the structure is not well-reproduced. Instead of a single, 183 intense peak, the red profile has a weaker, bimodal struc-184 ture. In addition, the bright region is much more extended 185 in the simulation than the experiment. One explanation 186 for the discrepancy comes directly from the experimental 187 image: A localized bright region inside the shock wave is 188 indicative of a strong density gradient which would "de-189 flect" photons from the higher density region to the lower 190 one. This single intensity peak is probably due to the rar-191 efaction wave which stands behind the shock front and in-192 side the shocked material. Moreover the strong 2D evolu-193 tion observed is more consistent with a smaller focal spot. 194 We could not characterize the focal spot at full power and 195 there was no phase plate to smooth the focal spot distri-196 bution. It is therefore reasonable to expect high intensity 197 spikes which would affect laser energy deposition. In addi-198 tion, considering the wavelength used, we were also more 199 susceptible to parametric effects which could modify the 200 energy absorption. 201

To test this hypothesis, we performed several simula-202 tions where we progressively reduced the laser spot size 203 from 50 μ m down to a 5 μ m central spike. Results for 204 the smallest focal spot are detailed in Figure 3c. Here, 205 we can distinguish a bright region corresponding to a sin-206 gle phase-contrast peak that is broadly consistent with 207 our experimental results. While the agreement is not per-208 fect, this simulation proves that a spike in laser intensity 209 can dramatically affect the resulting phase-contrast image. 210 The laser energy was kept at 25 J in these simulations. In 211 Figure 4b, we present on-axis intensity profiles for the ex-212 periment alongside numerical simulations with a smaller 213 focal spot. A single, intense peak is apparent in the central 214 region that is qualitatively consistent with the experiment. 215 One explanation for a smaller focal spot in our experiment 216 could be self-focusing of the laser beam [32, 33]. The laser 217 pulse duration was long ($\tau = 2$ ns), which would allow 218 the laser to interact with plasma generated earlier in the 219 interaction. In order to improve the agreement, a more 220 detailed characterization of the focusing condition is re-221 quired. Moreover, the experimental image 3a shows a non 222 uniform curvature radius of the shock front. This suggest 223 that we should treat this as a three dimensional problem. 224

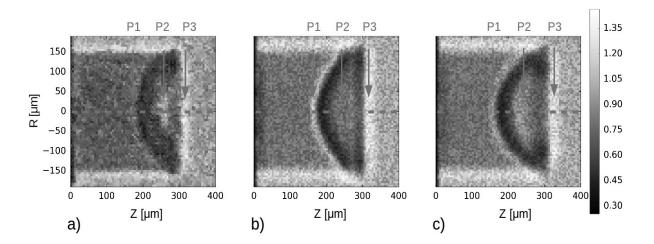


Fig. 3: Comparison between a) XPCI from the experiment, b) A synthetic XPCI image calculated using a specific module coupled to the DUED hydrodynamic code using the nominal focal spot and c) The synthetic XPCI image, using a small focal spot. A numerical noise was added to the images b) and c) according to the experimental measurement.

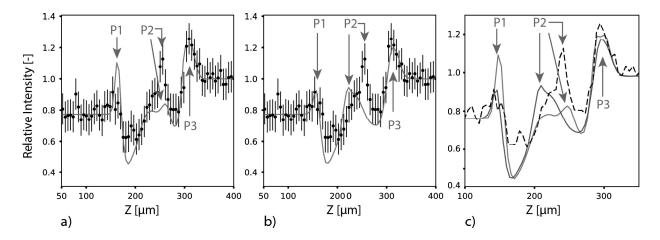


Fig. 4: Comparison between the profile along the propagation axis of a) XPCI simulation with nominal focal spot dimension, b) reduced focal spot dimension. Image c) shows the profile comparison between the simulations (red and blue lines) with the experiment (black dashed line).

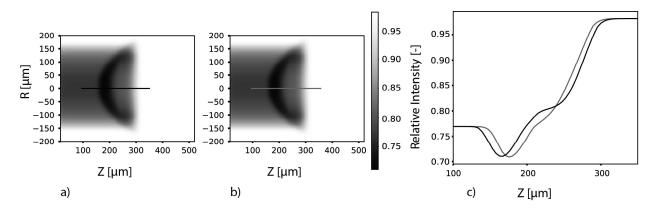


Fig. 5: Synthetic radiographs corresponding to the simulation with a) nominal focal spot and b) reduced focal spot. The image c) compares the intensity profiles along the axis of the image a) (black line) and b) (red line).

286

291

292

296

297

298

299

300

301

302

305

306

307

308

309

310

311

312

313

314

315

316

317

318

319

320

321

322

323

324

325

329

330

331

332

distribution inside the focal spot. However the high qual-226 ity XPCI images allow a detailed study of the shock shape. 227 By contrast, X-ray absorption radiography does not pro-228 vide us with the same level of detail. To prove this, we 229 can compare the synthetic absorption radiography of the 230 two simulations. The results are shown in Figure 5a and 231 5b. It is much harder to identify differences between the 232 simulations using X-ray absorption than with phase con-233 trast imaging (cf. Figure 3b and 3c). In Figure 4c, we 234 show on-axis intensity profiles for the images in Figure 3b 235 and 3c. The red and black absorption profiles are similar, 236 but the red is slightly shifted with the suggestion of a cen-237 tral bump. The energy deposition is different in the two 238 cases and this can cause a difference in the shock velocity. 239 In the case of a small focal spot (red), the 2D effects are 240 stronger and they cause energy to diffuse transverse to the 241 propagation axis. Figure 4 shows the same profile with the 242 phase contrast included. Even accounting for the low reso-243 lution of the detector (IP), the structure of the shock wave 244 and the rarefaction wave have been successfully observed. 245 Experimental work has already been done to compare ab-246 sorption radiography and XPCI in other contexts. In [28], 247 for example, X-ray imaging of a locust demonstrates that 248 XPCI is able to detect features that are completely absent 249 from images made using absorption radiography. The su-250 perior sensitivity of XPCI could open up new avenues in 251 the study of warm dense matter, laboratory astrophysics 252 or hydrodynamic instabilities at a variety of densities. 253

using a 3D code with a detailed knowledge of the energy

225

In this work we have presented new XPCI data from 254 the PHELIX laser system at GSI in Germany, using a 255 broadband X-ray source generated by a single laser beam. 256 Our set-up was first tested on static objects and then 257 used to image a laser-driven shock wave. In both cases, 258 phase-contrast at the density interfaces could be clearly 259 discerned. The intrinsic sensitivity of XPCI to density 260 gradients enabled us to observe subtle details in the struc-261 ture of the shock wave even at low X-ray flux (only 25 J in 262 the backlighter). At larger facilities, where more energetic 263 backlighter beams produce higher X-ray fluxes, the quality 264 of the data would be significantly improved (the signal-to-265 noise ratio would increase). XPCI is more sensitive to 266 density gradients than X-ray absorption radiography and 267 works well with polychromatic sources. This experiment 268 proved that XPCI can be a useful tool in studies of warm 269 dense matter and high energy density physics, paving the 270 way for testing on large-scale laser facilities. 271

* * *

This work has been carried out within the framework of the EUROfusion Enabling Research Project: AWP17-ENR-IFE-CEA-01 "Preparation and Realization of European Shock Ignition Experiments" and has received funding from the Euratom research and training programme 2014-2018 under grant agreement No 633053. The views and opinions expressed herein do not necessarily reflect those of the European Commission. The research leading to these results has received funding from LASERLAB-EUROPE (grant agreement no. 654148, European Union's Horizon 2020 research and innovation programme). The authors thanks Dr D Bleiner for having contributed to the purchase of a few targets used in the experiment described in this paper. 229

REFERENCES

- [1] SCHROPP A., ET AL., Scientific reports, 5 (2015) 11089. 287
- HAWRELIAK J., ERSKINE D., SCHROPP A., GALTIER
 E.C., AND HEIMANN P., AIP Conference Proceedings, 289
 1793 (2017) 090006. 290
- [3] NAGLER B., ET AL., Journal of synchrotron radiation, 22 (2015) 520-5.
- [4] FOURMAUX S., ET AL., Optics letters, **36** (2011) 2426-8. 293
- [5] KNEIP S., ET AL., Applied Physics Letters, 99 (2011) 294 093701.
- [6] DAVIS T.J., GAO D., GUREYEV T.E., STEVENSON A.W., AND WILKINS S.W., *Nature*, **373** (1995) 11089.
- [7] SNIGIREV A., SNIGIREVA I., KOHN V., KUZNETSOV S., AND SCHELOKOV I., Review of scientific instruments, 66 (1995) 5486-92.
- [8] MOMOSE A., TAKEDA T., ITAI Y., AND HIRANO K., Nature medicine, 2 (1996) 473-5.
- [9] WILKINS S.W., GUREYEV T.E., GAO D., POGANY A., AND STEVENSON A.W., *Nature*, **384** (1996) 335.
- [10] MILLER G.H., MOSES E.I., AND WUEST C.R., Optical Engineering, 43 (2004) 2841-54.
- [11] FLEUROT N., CAVAILLER C., AND BOURGADE J.L., Fusion Engineering and Design, 74 (2005) 147-54.
- [12] FLEUROT N., CAVAILLER C., AND BOURGADE J.L., Journal of Physics: Conference Series, 244 (2010) 032003.
- [13] BATANI D., HULIN S., DUCRET J.E., AND DHUMIERES E., Acta Polytechnica, 53 (2013) 37.
- [14] BENUZZI-MOUNAIX A, ET AL., Plasma physics and controlled fusion, 48 (2006) B347.
- [15] LE PAPE S, ET AL., Review of Scientific Instruments, 79 (2008) 106104.
- [16] ANTONELLI, ET AL., *Physical Review E*, **95** (2017) 063205.
- [17] ANTONELLI, ET AL., Journal of Instrumentation, 79 (2018) C01013.
- [18] KRITCHER A.L., ET AL., High Energy Density Physics, 10 (2014) 27-34.
- [19] DEL SORBO D., ET AL., Laser and Particle Beams, 33 (2015) 525-34.
- [20] MORACE A., ET AL., *Physics of Plasmas*, **21** (2014) 102712.
- WORKMAN J., COBBLE J., FLIPPO K., GAUTIER D.C., MONTGOMERY D.S., AND OFFERMANN D.T., Review of scientific instruments, 21 (2010) 10E520.
- [22] MONTGOMERY D.S., NOBILE A., AND WALSH P.J., Review of scientific instruments, 75 (2004) 3986-8.
- [23] NEUMAYER P., ET AL., Laser and Particle Beams, 23 (2005) 385-9.
- [24] SCHÖNLEIN A., ET AL., EPL (Europhysics Letters), 114 (2016) 45002.
 334
- [25] WU X., AND LIU H., Medical physics, **30** (2003) 2169-79. 335
- [26] COWLEY J.M., Diffraction physics, edited by ELSEVIER, 336
 Vol. 9 1995, p. 481. 337

- [27] OLIVO A., AND SPELLER R., *Physics in Medicine & Biology*, **51** (2006) 3015.
- [28] ARFELLI F., ET AL., Physics in Medicine & Biology, 43
 (1998) 2845.
- J. H. HUBBELL AND S. M. SELTZER, National Institute of Standards and Technology, Report No. NISTIR 5632
 (1995) (unpublished).
- [30] ATZENI S., ET AL., Computer physics communications,
 169 (2005) 153-9.
- ³⁴⁷ [31] FUJIOKA S., ET AL., hysics of Plasmas, 10 (2003) 4784 ³⁴⁸ 89.
- [32] YOUNG P.E., HAMMER J.H., WILKS S.C., AND KRUER
 W.L., *Physics of Plasmas*, 2 (1995) 2825-34.
- [33] YOUNG P.E., BALDIS H.A., DRAKE R.P., CAMPBELL
 E.M., ESTABROOK K.G., *Physical review letters*, 61 (1988) 2336.